International Journal of Biological Macromolecules 124 (2019) 377–388

Contents lists available at ScienceDirect

International Journal of Biological Macromolecules

journal homepage: http://www.elsevier.com/locate/ijbiomac

Fucosylated chondroitin sulfate from *Isostichopus badionotus* alleviates metabolic syndromes and gut microbiota dysbiosis induced by high-fat and high-fructose diet

Shan Li [a], Junhui Li [a], Guizhu Mao [a], Tiantian Wu [a], Dingbo Lin [b], Yaqin Hu [a], Xingqian Ye [a], Ding Tian [a], Wengang Chai [c], Robert J. Linhardt [d], Shiguo Chen [a,*]

[a] College of Biosystem Engineering and Food Science, Zhejiang University, Hangzhou 310058, China
[b] Department of Nutritional Sciences, Oklahoma State University, Stillwater, OK 74078, USA
[c] Glycosciences Laboratory, Department of Medicine, Imperial College London, Hammersmith Campus, London, W12 0NN, United Kingdom
[d] Center for Biotechnology and Interdisciplinary Studies, Rensselaer Polytechnic Institute, Troy, New York 12180, USA

ARTICLE INFO

Article history:
Received 26 October 2018
Received in revised form 12 November 2018
Accepted 17 November 2018
Available online 19 November 2018

Keywords:
Fucosylated chondroitin sulfate from sea cucumber
Metabolic syndromes
Gut microbiota
High-fat and high-sucrose diet

ABSTRACT

Fucosylated chondroitin sulfate from *Isostichopus badionotus* (fCS-*Ib*) is a kind of sulfated polysaccharides with well-repeated structure. In our former publications, fCS-*Ib* has been reported to be a functional food ingredient with hypoglycemic and antilipemic activities. However, there is no systematic study to investigate the effects of fCS-*Ib* on metabolic syndromes. In the present study, C57BL/6 mice fed on a high-fat and high sucrose diet (HFSD) for 6 weeks was used to cause metabolic syndromes. The final results showed that fCS-*Ib* alleviated obesity, hyperlipidemia, hyperglycemia, inflammation, liver steatosis, and adipocyte hypertrophy caused by HFSD. Meanwhile, fCS-*Ib* showed powerful effects on moderating gut microbiota dysbiosis in the HFSD-fed mice. Supplement of fCS-*Ib* could reduce ratio of Firmicutes to Bacteroidetes by decreasing abundance of Lachnospiraceae and *Allobaculum* while increasing abundance of Porphyromonadaceae, *Barnesiella*, and *Bacteroides*. Our results showed that fCS-*Ib* could be further developed as a potential pharmaceutical agent to prevent metabolic syndromes and gut microbiota dysbiosis.

1. Introduction

The metabolic syndromes (MetS), including obesity, dyslipidaemia, hyperglycaemia, and hypertension, have become one of the major public-health challenges worldwide [1]. It has been stated that environmental factors, particularly nutrition, act to program the risks for onset of metabolic syndromes [2]. To explore possible therapeutic measures, many experimental animal models fed on diets with increased total caloric intake have been used to result in metabolic syndromes [3]. These kinds of diets are typical features of what we call the "Western diet", which include excess saturated fatty acids and trans fats or simple sugars, such as fructose or sucrose. When the chime containing a lot of saturated fats and sugar flows into gut, a series of metabolic syndromes will appear. Firstly, the diversity and composition of gut microbiota will be influenced by over nutrition. Especially, high-fat diet (HFD) may sharpen the diversity and increase the ratio of *Firmicutes* to *Bacteroidetes* as well as pathogenic bacterium [4]. Another consequence of over nutrition is that when excessive nutrients flood into inner circulation, the functions of certain organs and tissues will be disturbed, especially for livers and adipose. Meanwhile, a whole inflammatory response will be induced, which is a key initiator of obesity and insulin resistance development [5].

Functional foods from natural sources are potential choices for addressing metabolic syndromes as they provide many health benefits with a low level of adverse side effects [6]. Polysaccharides, important universal components of life, are present in all plants, animals, and microorganisms [7]. Polysaccharides are multi-functional and these functions have been highlighted in many recent reviews [8,9], making these potentially important functional food ingredients. One of the remarkable activities reported for polysaccharides is their ability to regulate metabolic syndromes and related diseases, such as alleviating obesity, hyperlipidemia, hyperglycemia, insulin resistance, and chronic inflammation [10]. Remarkably, the effects of polysaccharides on gut microbiota have been emphasize in recent publications, which may be the key target to prevent metabolic syndromes [11].

Sulfated polysaccharides from sea cucumbers have escalated because of their unique structures with well-repeated units. There are mainly two kinds of sulfated polysaccharides in sea cucumbers, named as fucoidan and fucosylated chondroitin sulfate, respectively [12]. Fucosylated chondroitin sulphates from sea cucumbers, as important marine-derived sulfated polysaccharides, have been well studied

* Corresponding author.
E-mail address: chenshiguo210@163.com (S. Chen).

https://doi.org/10.1016/j.ijbiomac.2018.11.167
0141-8130/

for their anticoagulation activity [13,14]. The ability of fucosylated chondroitin sulfate (fCS) from sea cucumber to regulate energy metabolism was also reported. They can normalize glucose metabolism damaged by HFSD through PI3K/PKB/GSK-3β insulin signaling cascade in liver [15], PKB/GLUT4 signaling in skeletal muscle [16], PI3K/PKB/GLUT4 and ERK/GLUT4 signaling cascade in adipose tissue [17]. Recently, sulfated polysaccharides from *Stichopus japonicas* had been reported that they can prevent diet-induced obesity and its associated diseases by modulating the gut microbiota [18]. In our former study, fucosylated chondroitin sulfate extracted from *Isostichopus badionotus* (fCS-*Ib*) relatively with well-defined repeating oligosaccharide units has been reported to have powerful hypolipidemic activities [19]. As shown in the Supplementary Fig. 1a, fCS-*Ib* contains a chondroitin sulfate E (CSE) backbone, which is made up by repeating disaccharide units of alternating [4GlcAβ1-3GalNAc (4,6S) β1]. In CSE, the GalNAc is sulfated at both 4- and 6-positions. A single fucose as the branch was linked to the 3-position of the GlcA. Fucose branch in fCS-*Ib* is 2,4-*O*-sulfated [20]. However, the effects of this sulfated polysaccharide on the metabolic syndromes and gut microbiota are still unclear. In the present study, we focus our investigation on the multi-function of fCS-*Ib* including lipid profile, inflammation, liver function, and gut microbiota in the mice fed on a high-fat and high-sucrose diet (HFSD).

2. Materials and methods

2.1. Materials

Sea cucumbers *Isostichopus badionotus* (from Western Atlantic Ocean) were purchased from a local market in Qingdao, Shandong, China.

2.2. Preparation of sea cucumber polysaccharides

Crude sea cucumber polysaccharide was prepared based on a previously described method [21]. The crude fucosylated chondroitin sulphate from *I. badionotus* (fCS-*Ib*) was purified according to our former methods [22]. The molecular weight of fCS-*Ib* was determined by a high performance size exclusion chromatography (HPSEC) system according to the method described by Guo with some modifications [23]. The average Mw determination of fCS-*Ib* was performed on a Waters 1525 HPLC system (Waters, Milford, USA) with ultrahydrogel 2000 Column (7.8 × 300 mm) (Waters, Milford, USA). Forty microliters of the (2.0 mg/mL) were injected and eluted by 0.2 M NaCl at a flow rate of 0.5 mL/min. The standard dextrans of 80.90, 147.60, 273.00, 409.80 and 667.80 kDa were used to obtain the calibration curves for fCS-*Ib* calculated by Breeze 2 software. According to the standard curve, the final molecular weight of fCS-*Ib* was 10.9 kDa. The HPSEC profile of fCS-*Ib* was shown in Supplementary Fig. 1b and its chemical composition was shown in Supplementary Table 3.

2.3. Animals and experimental design

Thirty-two male C57BL/6J mice were purchased from the Shanghai Slaccas Laboratory Animal Company (Certificate Number SCXK (hu) 2007-0005, Shanghai, China). The mice were housed in ventilated cages within a pathogen-free barrier facility that maintained a 12-h light: 12-h dark cycle, and allowed to take water and food ad libitum. After 1 week for adaptation to the laboratory environment, animals were randomly divided into four groups with eight mice in each group. Group 1: mice were fed on regular chow and administered with distilled water by metallic gavage needle every day, named as the control group. Group 2: mice were fed on a HFSD (49.5% common chow + 15% sucrose + 20.4% lard + 12.3% protein + 2% premix compound + 0.8% maltodextrin) and administered with distilled water by metallic gavage needle every day, named as the HFSD group. Group 3: mice were fed on HFSD and administered with fCS-*Ib* solution dissolved in distilled water at a dose of 20 mg/kg/day by metallic gavage needle, named as the fCS-*Ib*-L group. Group 4: mice were fed on HFSD and administered with fCS-*Ib* solution dissolved in distilled water at a dose of 40 mg/kg/day by metallic gavage needle, named as the fCS-*Ib*-H group. The food consumption and weight gain were measured once a week. The Zhejiang University Standing Committee on Animals approved all mouse protocols.

After 6 weeks, the mice were withheld food for 12 h, weighed and blood samples were collected from their eyeballs. Serum, liver, kidney, white adipose tissue and colonic contents were collected, weighted, and frozen at −80 °C. A small part of liver and epididymal fat tissues were fixed on neutral formalin solution for histology.

2.4. Biochemical analysis of serum

Serum TC, TG, HDL-C, LDL-C, glucose, TNF-α and IL-6 levels were measured by enzymatic colorimetric methods using commercial kits (R&D Systems, USA).

2.5. Liver and epididymal fat histology

The fresh liver and epididymal fat samples were rapidly dissected and the liver tissue sections were fixed by the immersion in a 4% neutral formalin solution at room temperature for 48 h. Furthermore, the samples were dehydrated through ascending grades of alcohol, clarified in benzene and embedded in low melting point paraffin wax. Sections (3 nm thick) were cut and stained with hematoxylin and eosin (H &E staining) for light microscopic examination [24]. All of these assays were performed in a blinded manner.

2.6. RT-qPCR analysis

Total RNA was isolated from adipose tissues using a total tissue TRIzol® Plus RNA Purification Kit (Invitrogen, America). Equal amounts of total RNA were used to synthesize cDNA with the Quant II fast RT kit (Tools, Taiwan). Quantitative real-time reverse-transcription PCR (RT–qPCR) was performed in triplicate using SYBR Green, 384-well plates and the CFX384 Touch Real-Time PCR System (Bio-Rad, USA). Each well was loaded with a total of 20 μl containing 1 μl of cDNA, 1 μl of target primers, and 8 μl of SDW and 10 μl of Power SYBR® Green Master Mix. Hot-start PCR was performed for 40 cycles, with each cycle consisting of denaturation for 15 s at 94 °C, annealing for 30 s at 60 °C and elongation for 30 s at 72 °C. The housekeeping gene 18sRNA was used as a control. PCR products were quantitated using the software

Table 1
Effect of fCS-*Ib* on body weight in HFD-fed mice.

Groups	Initial weight (g)	1st week (g)	2nd week (g)	3rd week (g)	4th week (g)	5th week (g)	Final weight (g)	Gain weight (g)
Control	24.6 ± 1.3	24.7 ± 1.1	25.6 ± 1.2	25.6 ± 0.9	26.4 ± 1.1	26.4 ± 1.2	26.9 ± 0.9	2.3 ± 0.6*
HFSD	24.5 ± 1.5	26.1 ± 1.2	27.1 ± 1.3	27.3 ± 1.1	27.8 ± 1.2	28.1 ± 1.5	28.9 ± 0.9	4.4 ± 0.9#
fCS-*Ib*-L	25.1 ± 0.7	25.4 ± 1.1	26.0 ± 1.2	26.2 ± 1.3	26.6 ± 1.2	27.0 ± 1.7	27.7 ± 1.5	2.6 ± 0.8*
fCS-*Ib*-H	24.3 ± 1.2	25.4 ± 0.9	26.5 ± 1.1	26.2 ± 1.2	26.8 ± 1.2	26.9 ± 1.4	27.0 ± 1.3	2.6 ± 0.6*

Data are presented as mean ± SD, $n = 8$. The control group was supplied with common commercial chow and all the other groups were supplied with HFD.
* $P < 0.05$: compared with HFD group.
# $P < 0.05$: compared to normal control group

iCycler iQ5 (Bio-Rad, USA). The mRNA relative expression levels were expressed as the ratio of signal intensity for the target genes to that of 18sRNA [25]. The primers of related genes were shown in the Supplementary Table 1.

2.7. 16S rDNA analysis

DNA was extracted from the colon contents of mice by using the E.Z.N.A. ®Stool DNA Kit (D4015, Omega, Inc., USA) according to manufacturer's instructions. The reagent which was designed to uncover DNA from trace amounts of sample has been shown to be effective for the preparation of DNA of most bacteria. Nuclear-free water was used for blank. The total DNA was eluted in 50 μl of elution buffer and stored at −80 °C until measurement in the PCR by LC-Bio Technology Co., Ltd., Hang Zhou, Zhejiang Province, China. The 16S rDNA gene (V3 and V4 regions) from the colon microbiota was amplified using the universal primers as follows: 319F (5′-ACTCCTACGGGAGCAG-3′) and 806R (5′-GGACTACCAGGGTATCTAAT-3′) [26]. The PCR reactions were carried out in an ABI GeneAmp PCR System 9700 (Applied Biosystems, Foster City, USA). The amplicons were purified using the AxyPrep DNA gel extraction kit (Axygen Bioscience, Union City, USA) and quantified by a Promega Quantifluor® ST fluorometer (Promega, Madison, USA) before being sequenced on an Illumina MiSeq PE250 platform by Shanghai Majorbio Bio-pharm Biotechnology Co., Ltd. (Shanghai, China).

Samples were sequenced on an Illumina MiSeq platform according to the manufacturer's recommendations, provided by LC-Bio. Paired-end reads were assigned to samples based on their unique bar code and truncated by cutting off the bar code and primer sequence. Paired-end reads were merged using FLASH. Quality filtering on the raw tags was performed under specific filtering conditions to obtain the high-quality clean tags according to the FastQC (V 0.10.1). Chimeric sequences were filtered using Verseach software (v2.3.4). Sequences with ≥97% similarity were assigned to the same operational taxonomic units (OTUs) by Verseach (v2.3.4). Representative sequences were chosen for each OTU, and taxonomic data were then assigned to each representative sequence using the RDP (Ribosomal Database Project) classifier. The differences of the dominant species in different groups, multiple sequence alignment were conducted using the PyNAST software to study phylogenetic relationship of different OTUs. OTUs abundance information were normalized using a standard of sequence number corresponding to the sample with the least sequences. Alpha diversity is applied in analyzing complexity of species diversity for a sample through 4 indices, including Chao1, Shannon, Simpson and Observed species. All these indices in our samples were calculated with QIIME (Version 1.8.0). Beta diversity analysis was used to evaluate differences of samples in species complexity. Beta diversity was calculated by principle co-ordinates analysis (PCoA) and cluster analysis by QIIME software (Version 1.8.0). Linear discriminant analysis (LDA) effect size (LEfSe) analysis was performed to identify the dimensional gut bacteria and characterize the microbial differences between different treatment groups [27]. The Kruskal-Wallis rank sum test was applied to detect features that were significantly different between assigned taxa and the LDA was used to quantify the effect size of each feature. A significance alpha value of <0.05 and an effect size threshold of 2 were used for this analysis.

2.8. Statistical analysis

All experimental results are given as mean ± standard deviation (SD). Data obtained were analysed using one-way analysis of variance (ANOVA) and Duncan's multiple range tests. The level of statistical significance was set at $P < 0.05$.

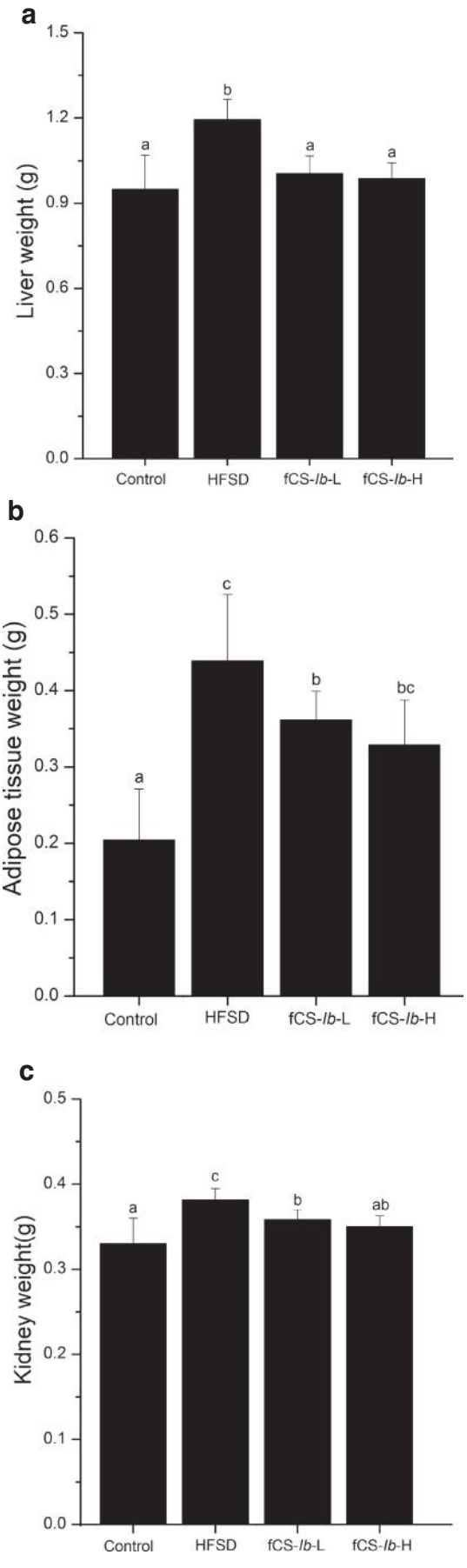

Fig. 1. Effects of fCS-*Ib* on the liver weight (a), epididymal fat weight (b), and kidney weight (c). All data are expressed as mean ± SD (n = 8). a, b, c: $P < 0.05$, the different letters represent significant differences between different groups.

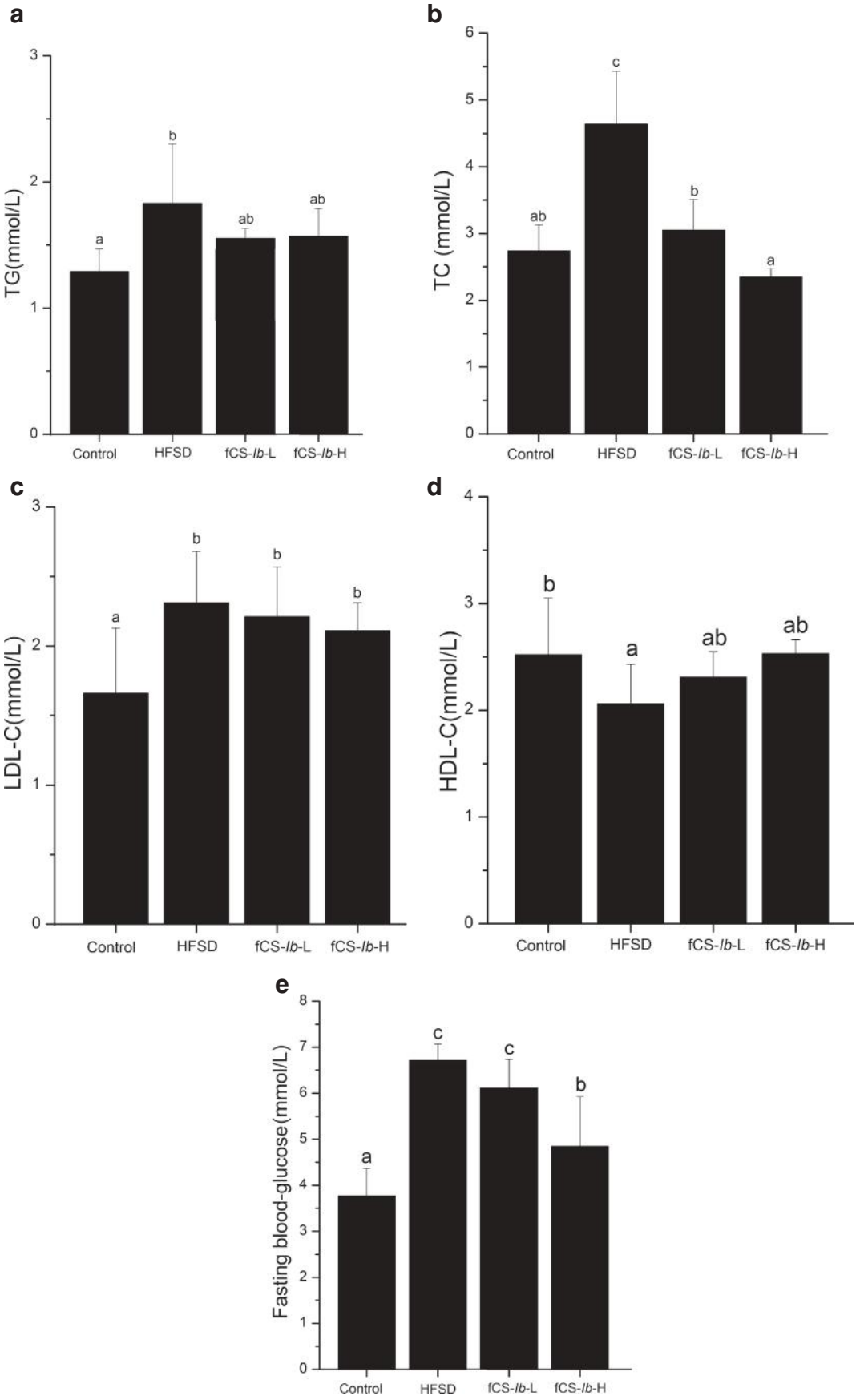

Fig. 2. Effects of fCS-*lb* on the serum TG (a), TC (b), LDL-C (c), HDL-C (d), and fasting blood glucose (e) on HFD-fed mice. All data are expressed as mean ± SD (n = 8). a, b, c: $P < 0.05$, the different letters represent significant differences between different groups.

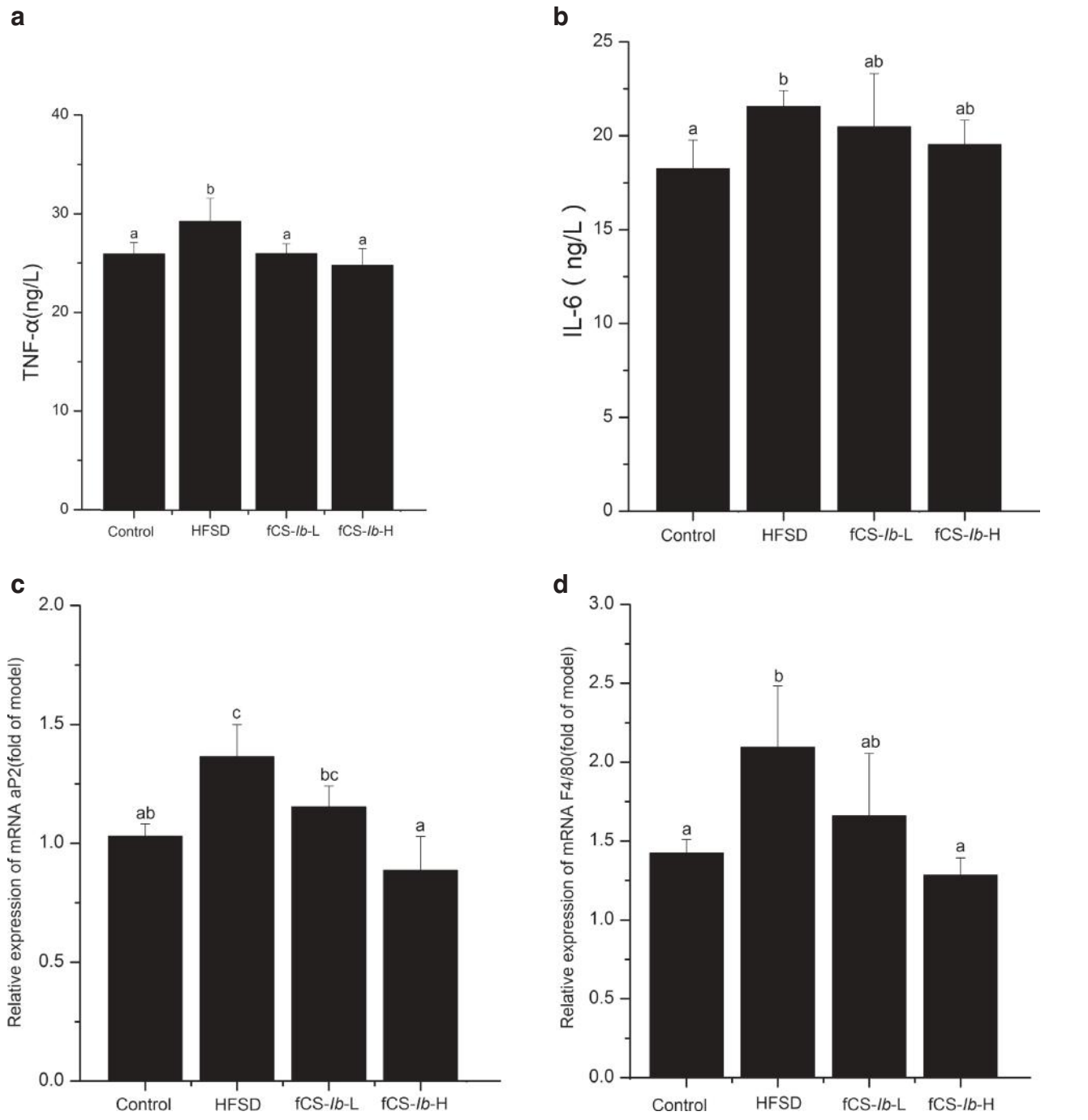

Fig. 3. Effects of fCS-*Ib* on the serum TNF-α (a) and IL-6 (b), on HFD-fed mice. Data of TNF-α and IL-6 are expressed as mean ± SD (n = 8). Effects of fCS-*Ib*, DfCS-*Ib* on aP2 (c) and F4/80 (d) of adipose tissues using qRT-PCR, and the results were normalized by18s rRNA. Data of qRT-PCR are expressed as mean ± SD ($n = 4$). a, b, c: $P < 0.05$, the different letters represent significant differences between different groups.

3. Results

3.1. Effects of fCS-Ib on obesity caused by HFSD

In the present study, a combination of 15% sucrose and 20.4% lard was used to establish metabolic syndromes. The body weights of four groups during the experimental period are presented in the Table 1. From the first week, the mice in the HFSD group got more weight gains than the control group. After 6 weeks, HFSD feeding led to significant increases in body weight gains ($P < 0.05$, compared with the control group). Supplementation with fCS-*Ib* could significantly decreased weight gains in the mice fed on HFSD, and even the lower dosage of fCS-*Ib* at 20 mg/kg could significantly inhibit the abnormal weight gains ($P < 0.05$, compared with the HFD group). The liver weight (Fig. 1a), epididymal fat weight (Fig. 1b), and kidney weight (Fig. 1c) were also significantly increased in the mice fed on HFSD. Especially, the fCS-*Ib*-H group maintained the liver and kidney weight at normal levels ($P > 0.05$ compared with the control group). However, the effects of two fCS-*Ib* groups on epididymal fat weight were limited ($P < 0.05$ compared with the control group and the HFD group). Meanwhile, the

food consumption was not significantly different among all the four groups (data not shown). All data indicated that fCS-*Ib* could be potential functional food ingredient to prevent obesity.

3.2. Effects of fCS-Ib on hyperlipidemia and hyperglycemia caused by HFSD

International Diabetes Federation have defined that for a person to be defined as having the MetS, they must have central obesity plus any two of four additional factors (raised TG level, reduced HDL-C, raised blood pressure, and raised fasting plasma glucose) [1]. In our study, HFSD disturbed lipid profile by raising serum TG, TC and LDL-C levels while decreasing HDL-C level ($P < 0.05$ between the HFSD group and the control group), which was significantly restored by supplement with fCS-*Ib* (shown in the Fig. 2a-d). Meanwhile, the glucose level in the HFSD group was much higher than that of the control group ($P < 0.05$ between the HFSD group and the control group, shown in the Fig. 2e). Administration of fCS-*Ib* at dosage of 40 mg/kg/day resulted in a significant glucose-lowering effect ($P < 0.05$ compared with the HFSD group). The data in this part indicated fCS-*Ib* alleviated hyperlipidemia and hyperglycemia caused by HFSD in a dose–dependent way.

3.3. Effects of fCS-Ib on inflammation caused by HFSD

Inflammation is a risk factor contributing to a cluster of MetS, particularly obesity, type 2 diabetes and cardiovascular disease [28]. The influx of excessive nutrients into inner metabolism can trigger classical inflammatory pathways, such as the NF-κB signaling pathway, through activating downstream signaling of Toll-like receptors (TLRs) [29]. Activation of inflammatory pathways results in the production of pro-inflammatory cytokines such as IL-6, IL-1, and TNF-a. An assessment of the major cytokines (TNF-α and IL-6) produced after 6 weeks of the HFSD revealed a significant elevation compared with serum levels of mice in the control group ($P < 0.05$ compared with the control group, shown in the Fig. 3a and b). Both the fCS-*Ib*-L and fCS-*Ib*-H groups significantly depressed the serum TNF-α level ($P < 0.05$ compared with the HFSD group). The serum IL-6 level was also decreased by supplement

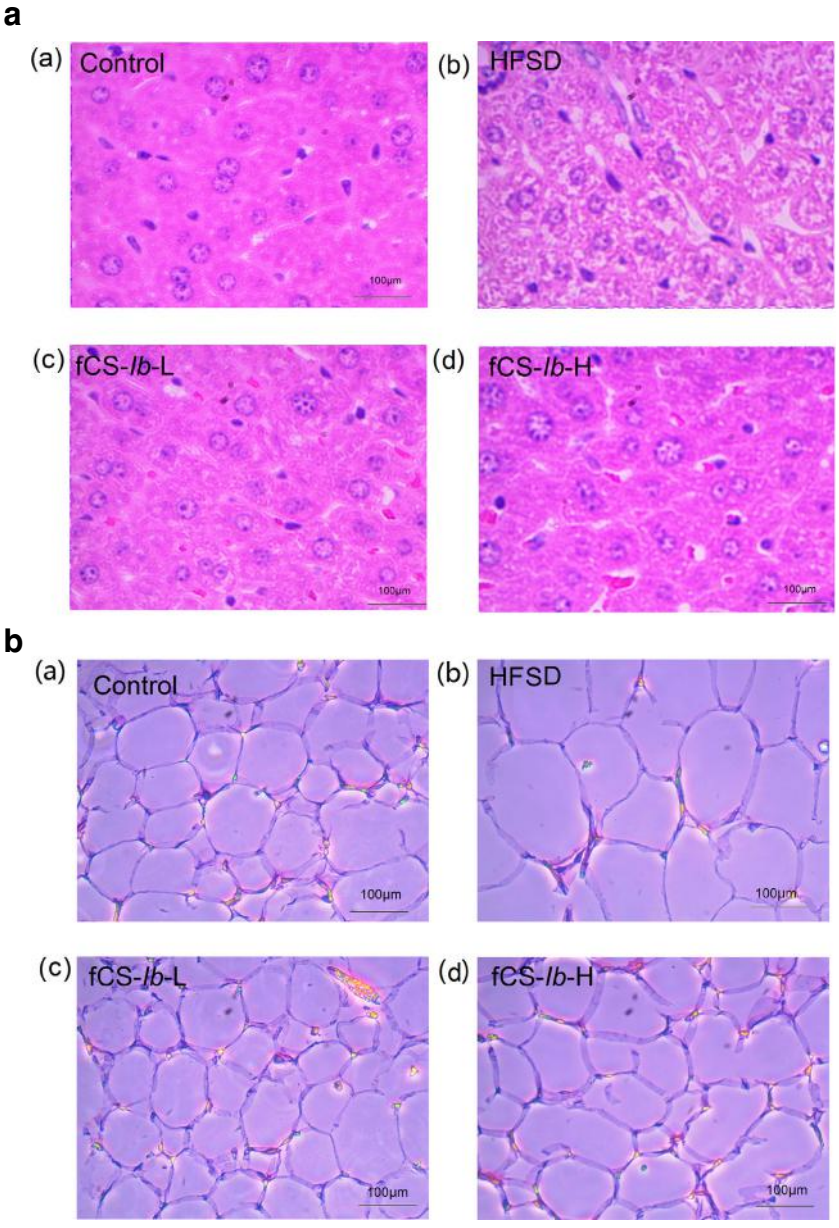

Fig. 4. a histological assessment of livers in high fat diet-induced obesity mice(H&E stain, 200× magnification); b histological assessment of fat tissues in high fat diet-induced obesity mice (H&E stain, 200 × magnification).

with fCS-*Ib*, although significant differences were not observed ($P > 0.05$ compared with the HFSD group).

These inflammatory cytokines drive macrophage activation and propagation of pro-inflammatory signals throughout the organism, thus initiating parallel cascades of inflammatory reactions. The inflammatory state, caused by long term over nutrition, finally develops into a state of chronic unresolved inflammation [30]. Studies demonstrated that a key mechanism underlying obesity-induced inflammation is the accumulation of increased numbers of tissue macrophages, particularly in obese adipose tissue [31]. Macrophages are present in much higher numbers in adipose tissue of obese subjects than in that of lean subjects and appear to be major sources of inflammatory mediators such as TNF-α [32]. As shown in the Fig. 3c and d, we measured the mRNA expression of aP2 and F4/80 in the adipose tissue to investigate the degree of macrophages infiltrating into adipose tissue. The adipocyte fatty acid-binding protein, aP2, has been considered as an adipocyte-specific protein. However, it has been found to be expressed in macrophages and involved in metabolic inflammation [33]. Mice with aP2 deficiency are protected from inflammation [34]. In our study, the expression of aP2 was significantly up-regulated by HFSD ($P < 0.05$ compared with the control group, Fig. 3c). In the fCS-*Ib*-L group, the expression of aP2 was down-regulated compared with the HFSD group. In the fCS-*Ib*-H group, the expression of aP2 was down-regulated in the adipose tissue of HFSD-fed mice, which was even lower than the control group. F4/80 is a specific macrophage marker [35]. As shown in the Fig. 3d, HFSD caused significantly increasing expression of F4/80 in the adipose tissue compared with that of the control group ($P < 0.05$). Supplement with enough fCS-*Ib* could efficiently decreased the expression of F4/80 ($P > 0.05$ between the fCS-*Ib*-L group and the control group). In conclusion, fCS-*Ib* could alleviate inflammation by decreasing serum inflammatory cytokines and dampening macrophages infiltrating into adipose tissue.

3.4. Effects of fCS-Ib on liver steatosis and adipocyte hypertrophy caused by HFSD

One of the consequences of over nutrition is the development nonalcoholic fatty liver disease (NAFLD) [36]. Histopathological observation of the liver was performed to investigate the effect of fCS-*Ib* on hepatic steatosis. Fig. 4a showed photomicrographs of H&E stained liver tissues. In comparison with hepatic cellular architecture of the normal mice, the HFSD led to severe enlargement of liver cell volume, the structural disorder of hepatic lobules, and large fat vacuoles. The morphological structures of hepatocytes in HFSD-fed mice were significantly recovered by treatment with fCS-*Ib*. Relatively normal structures of hepatic lobules and significantly improved fatty degeneration of liver cells were noted in both fCS-*Ib* groups. Our results indicated fCS-*Ib* could efficiently ameliorated hepatic steatosis caused by over nutrition.

The manifestation of obesity is being overweight due to TG accumulated in the adipose tissue. When adipose tissue is exposed to caloric abundance, it stores free fatty acids (FFAs) in the form of TG through esterification. Additional pre-adipocytes are driven to differentiate into white adipocytes, thus inducing fat hypertrophy. As shown in Fig. 4b, the size of adipocyte was enlarged by HFSD compared with the adipocyte in the control group. The supplement of fCS-*Ib* affected the development of adipocytes. Both the fCS-*Ib*-L group and the fCS-*Ib*-H group significantly reduced the adipose size of HFSD-fed mice. This result indicated that fCS-*Ib* can reduce lipid accumulation in adipose tissues, thus reducing body weight gains.

3.5. Effects of fCS-Ib on gut microbiota in HFSD-fed mice

The importance of gut microbiota for human health has been emphasized in the past decades [37]. One issue that has emerged in recent years is the link between metabolic syndromes and the composition and functionality of the gut microbiota [38]. Dietary changes in particular have been shown to have significant effects on the composition and diversity of gut microbiota. Especially, diets with excess energy contribute to increasing abundance of microorganisms that are related to metabolic diseases [37].

In this section, we investigated how fCS-*Ib* modulated the profiles of colonic microbiota in the HFSD-fed mice. Since both low and high dosages of fCS-*Ib* had profound effects on alleviating metabolic syndromes, the high dose of fCS-*Ib* was selected to investigate its effects on gut microbiota by 16S rDNA. Firstly, alpha diversity analysis was performed to value the richness and diversity of three groups. Former studies have reported that the diversity of gut microbiota could be sharpen by high-fat diet [39]. According to Simpson index (Fig. 5a) and observed species (Fig. 5b), bacterial diversity and richness were not changed by HFSD in the present study ($P > 0.05$, compared with the control group, Fig. 5a and b). FCS-*Ib* exerted almost no influence on bacterial diversity but increased richness in HFSD-fed mice. Venn diagram showed the similarity and specificity of operational taxonomy units (OTUs) in these three groups (Fig. 5c). The more OTUs were found in the fCS-*Ib* group compared with that of the control group and the HFSD group,

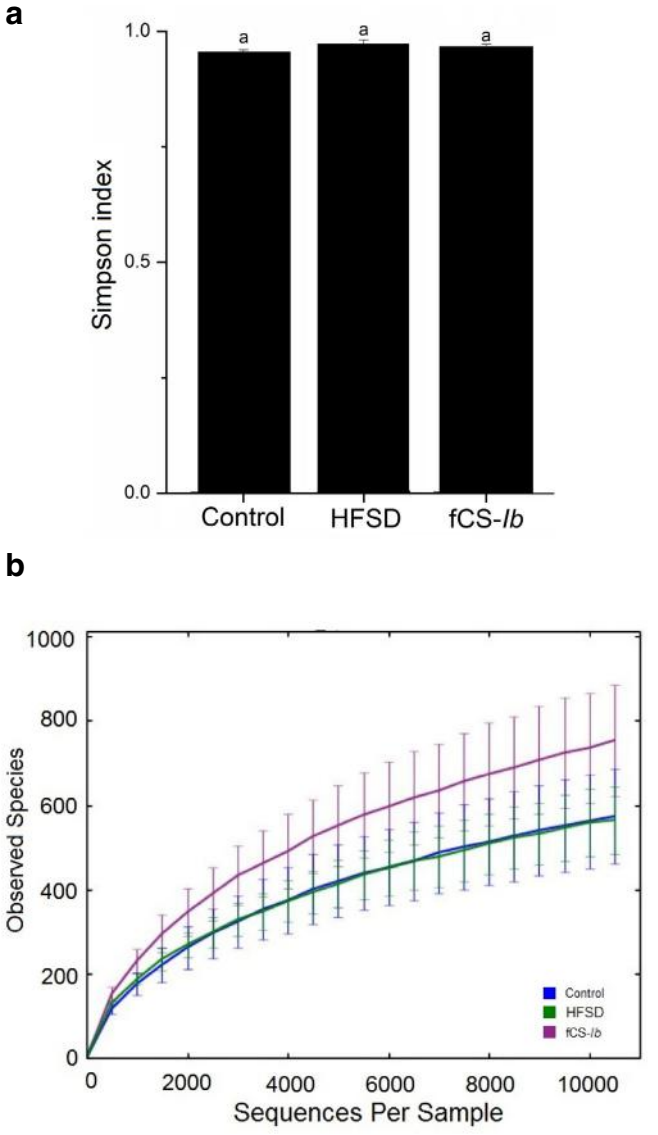

Fig. 5. Structural comparison of gut microbiota among control, HFD, fCS-*Ib*, *and* DfCS-*Ib* groups. Simpson index of the three groups (a). Observed species of the three groups Venn diagram comparison of OTUs in gut microbiota among the three groups (c). PCoA plot of gut microbiota based on weighted UniFrac metric (d).

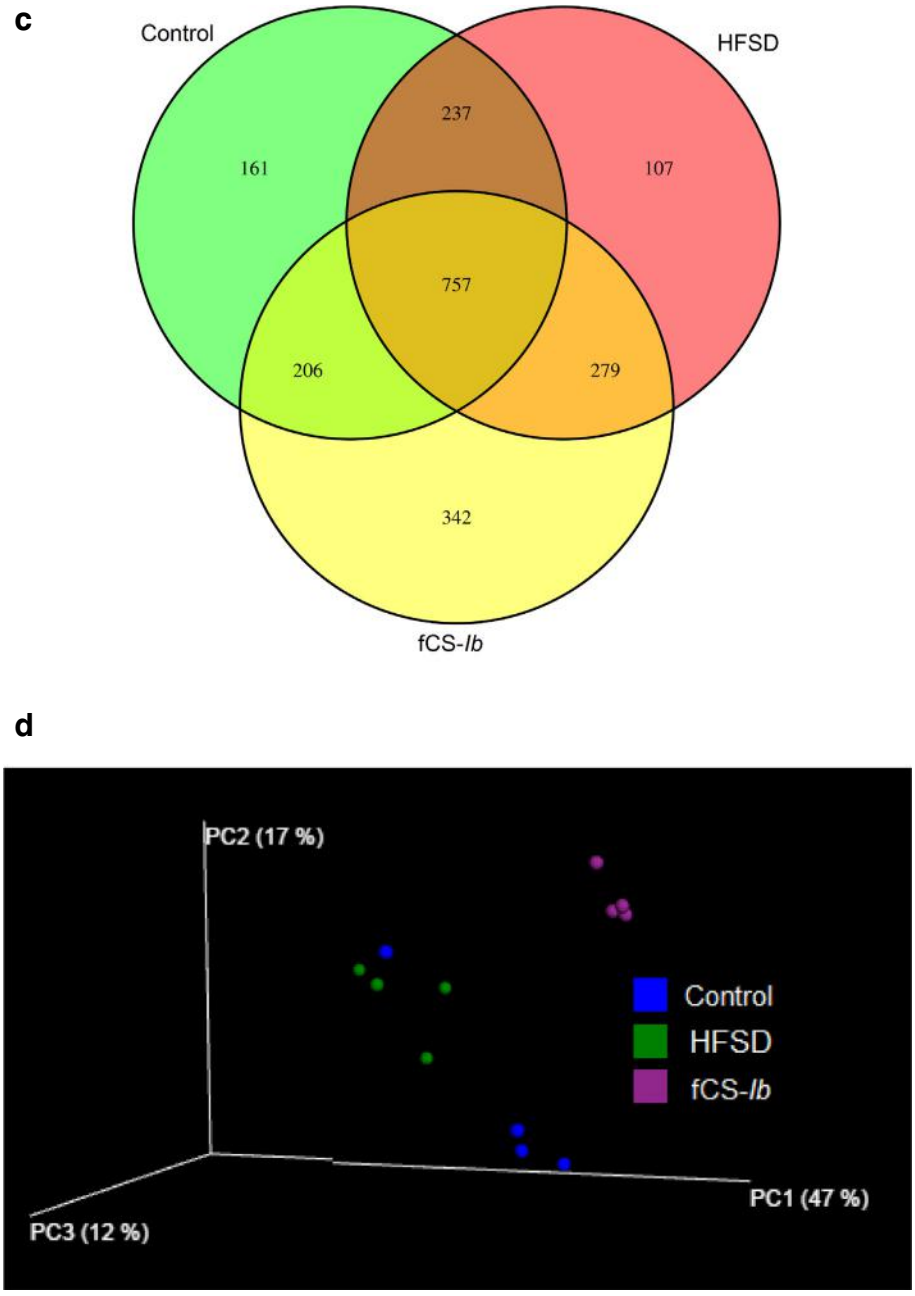

Fig. 5 (*continued*).

which indicated the powerful effects of fCS-*Ib* on gut microbiota. In addition, PCoA plot based on weighted UniFrac metric show a distinct clustering of gut microbiota compositions between the three groups (Fig. 5d). Combined all these results, the composition of gut microbiota induced by HFSD was distinct from that of the normal group. Supplement fCS-*Ib* changed the gut microbiota in the HFSD-fed mice. Meanwhile, the gut microbiota in the fCS-*Ib* group also had specific gut microbiota profile, which was different from that of the normal group.

Then, the composition of gut microbiota in the three groups with different treatments is discussed both at phylum and genus levels. Similar to the gut microbiota of human, it is dominated by Bacteroidetes and Firmicutes, whereas Actinobacteria, Proteobacteria, and Verrucomicrobia are frequent but generally minor constituents in mice [40]. According to results of the 16 s RNA (Fig. 6a), Bacteroidetes and Firmicutes are the dominant phylum in the three groups. The microbiota of mice fed with HFSD showed a significantly increased relative abundance of Firmicutes, and a decreased relative abundance of Bacteroidetes, Actinobacteria, and Verrucomicrobia compared with the microbiota of mice with the control group. Remarkably, HFSD increased the ratio of Firmicutes to Bacteroidetes from 0.37 (the ratio of F/B of the control group) to 1.18. FCS-*Ib* reversed the ratio of F/B to 0.28 in the HFSD-fed mice, a value even lower than the control group. FCS-*Ib* exerted no effects on reversing other microorganism at the phylum level. At the level (Fig. 6b), HFSD decreased the abundance of *Barnesiella*, while increased that of *Alistipes* and *Allobaculum* (compared to the control group). FCS-*Ib* increased the proportion of *Barnesiella* while decreased that of *Allobaculum* in the HFSD-fed mice. Meanwhile, the abundance of *Bacteroides* In fCS-*Ib* group was much higher than

other two groups. There was no significant change in the abundance of *Bacteroides* between the HFSD and control group. FCS-*Ib* supplement increased *Bacteroides* from 2.0% to 10.8% in HFD-fed mice.

Furthermore, LEfSe analysis was performed to compare the specific bacterium of the fCS-*Ib* group with the HFSD group including all microorganisms at different levels. Compared with the control group, the dominant bacterium in the HFD group was characterized by a higher amount of Firmicutes, Clostridia, Clostridiales Lachnospiraceae, and *Alistipes* and a lower amount of Bacteroidetes, Porphyromonadaceae, and *Barnesiella* (Fig. 6c and Supplementary 2a). In the fCS-*Ib* group,

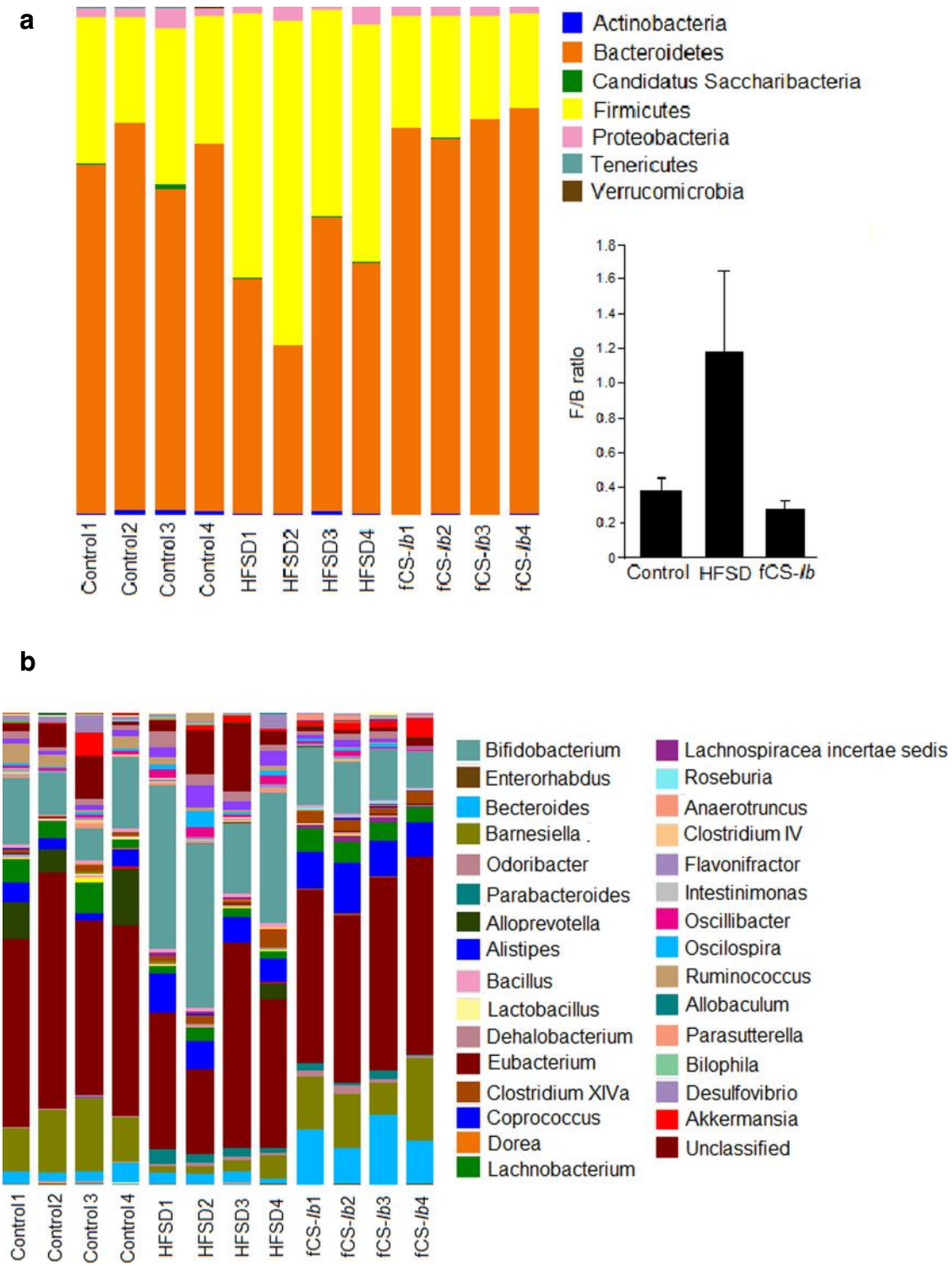

Fig. 6. Composition of gut microbiota in control, HFD, and fCS-*Ib* groups at phylum level (a); Composition of gut microbiota in control, HFD, and fCS-*Ib* groups at genus level (b); LEfSe comparison of gut microbiota between control and HFD groups (c); LEfSe comparison of gut microbiota between HFD and fCS-*Ib* groups (d).

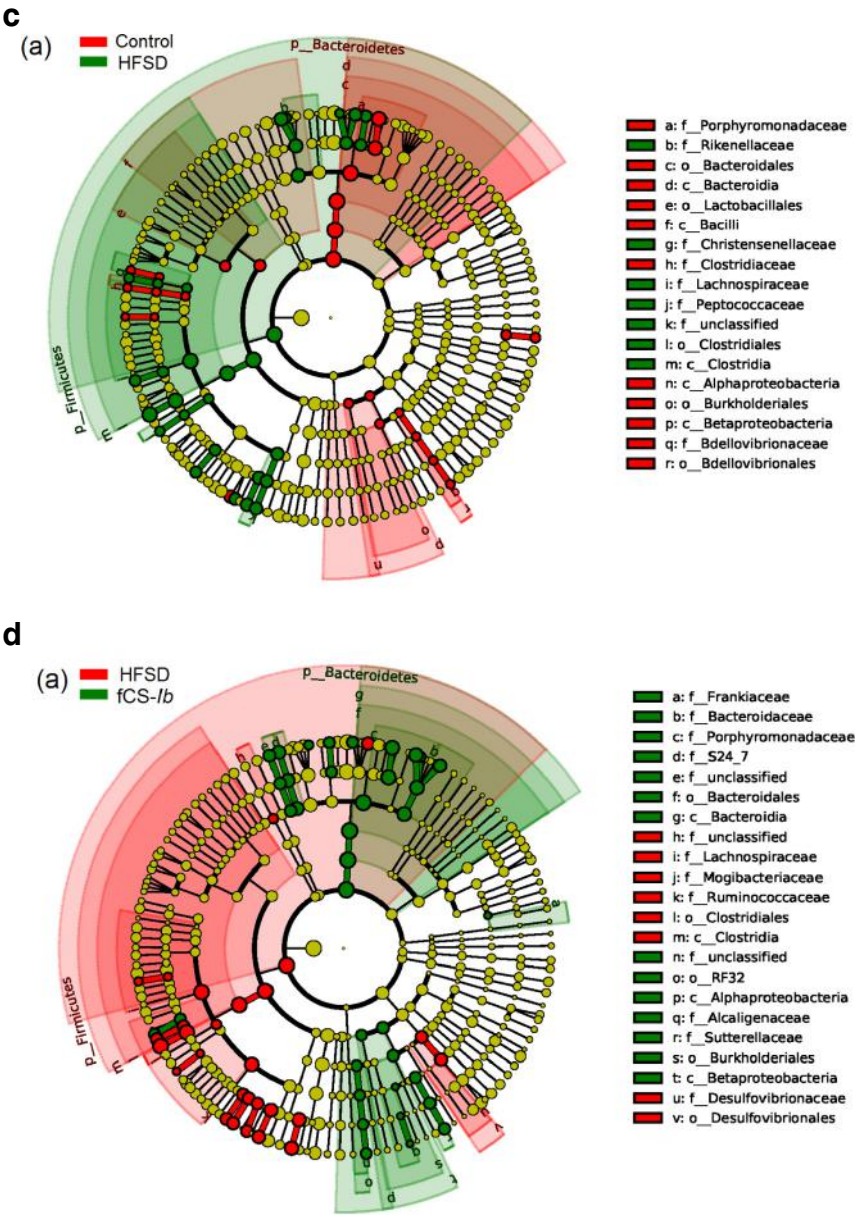

Fig. 6 (*continued*).

there were lower abundance of Firmicutes, Clostridia, Clostridiales Lachnospiraceae, and *Allobaculum* and higher abundance of Bacteroidetes, Porphyromonadaceae, and *Barnesiella* in HFSD-fed mice (Fig. 6d and Supplementary 2b).

Combined of all results of 16 s RNA, fCS-*Ib* reduced the relative abundance of Firmicutes by decreasing the relative abundance of Clostridia, Clostridiales, Lachnospiraceae, and *Allobaculum*. FCS-*Ib* improved the relative abundance of Bacteroidetes by increasing the relative abundance of Porphyromonadaceae, *Bacteroides* and *Barnesiella*. The view that an increased ratio of Firmicutes to Bacteroidetes at the phylum level could promote the development of obesity in mice has been reported in many publications [41,42]. Our results confirmed the idea that the ratio of F/B is positively correlated to obesity. It is noteworthy that fCS-*Ib* reversed the ratio of F/B to a normal level in HFSD-fed mice. However, HFSD had no effects on the relative abundance of Proteobacteria in the present work, which is not consistent with former studies that the relative increased abundance of Proteobacteria has been found in the mice fed on High-fat diet (HFD) [10]. High abundance of Lachnospiraceae bacteria (phylum Firmicutes, class Clostridia) has been found in HFD diet and is associated with metabolic syndromes, such as obesity, type 2 diabetes, inflammatory bowel disease [43]. We found that fCS-*Ib* decreased colonic *Allobaculum* to a very low abundance. *Allobaculum* is a kind of SCFAs-producing bacteria belonging to within the family Erysipelotrichaceae and the phylum Firmicutes [44]. However, the family Erysipelotrichaceae was controversial for the relationship between its abundance in the gut and inflammatory bowel diseases [45]. *Allobaculum* has been considered as a type of bacteria positively related to obesity in mice feeding on HFSD [46]. FCS-*Ib* supplement increased *Bacteroides* from 2.0% to 10.8% in HFD-fed mice. *Bacteroides* is one of members of the human gut microbiota that confer myriad benefits on their hosts [47]. FCS-*Ib* increased the abundance of *Barnesiella*, a genus belonging to the family Porphyromonadaceae and the phylum Bacteroidetes. The higher levels of *Barnesiella* in the colon are able to protect against the intestinal dominance of antibiotic-resistant pathogenic bacteria and correlate with the amount of several immune regulatory cells [48]. Our results of gut microbiota indicated

that fCS-*Ib* could restore the composition of gut microbiota in the HFSD-fed mice.

4. Conclusion

In the present work, the results of body weight gains, fat, liver, and kidney weight indicated that fCS-*Ib* could inhibit HFSD-fed mice from becoming obese. Meanwhile, fCS-*Ib* could reverse lipid profile, lower serum glucose level, and alleviate low-degree inflammation caused by HFSD. Furthermore, fCS-*Ib* showed powerful effects on reversing F/B value mainly through decreasing abundance of Firmicutes, Lachnospiraceae and *Allobaculum* while increasing abundance of Bacteroidetes, Porphyromonadaceae, *Bacteroides*, and *Barnesiella*. Our results indicated that fCS-*Ib* can be pharmaceutical agent for its specific effects on metabolic syndromes. However, more specific studies are needed to further decipher the effects of fCS-*Ib* on gut microbiota, especially intestinal flora related to metabolic syndromes.

Author contributions

Shiguo Chen and Shan Li conceived and designed the experiments; Shan Li, Junhui Li, Guizhu Mao, and Tiantian Wu performed the experiments; Robert John Linhardt and Dingbo Lin analysed the data; Shan Li and Robert John Linhardt wrote the paper; Tian Ding carried out the revision process.

Conflict of interest

The authors have declared no conflicts of interest.

Appendix A. Supplementary data

Supplementary data to this article can be found online at https://doi.org/10.1016/j.ijbiomac.2018.11.167.

Abbreviations

MetS	metabolic syndromes
fCS-*Ib*	Fucosylated chondroitin sulfate from *Isostichopus badionotus*
HFSD	high-fat and high-sucrose diet
TG	triglycerides
CSE	chondroitin sulfate E
GPC	gel permeation chromatography
HDL-C	high density lipoprotein cholesterol
LDL-C	low density lipoprotein cholesterol
TNF-α	tumor necrosis factor
IL-6	interleukin-6
aP2	adipocyte fatty-acid-binding protein
F/B	the ratio of Firmicutes and Bacteroidetes

References

[1] K.G.M. Alberti, P. Zimmet, J. Shaw, The metabolic syndrome—a new worldwide definition, Lancet 366 (9491) (2005) 1059–1062.
[2] I.C. Mcmillen, J.S. Robinson, Developmental origins of the metabolic syndrome: prediction, plasticity, and programming, Physiol. Rev. 85 (2) (2005) 571.
[3] S. Aydin, A. Aksoy, S. Aydin, M. Kalayci, M. Yilmaz, T. Kuloglu, C. Citil, Z. Catak, Today's and yesterday's of pathophysiology: biochemistry of metabolic syndrome and animal models, Nutrition 30 (1) (2014) 1–9.
[4] B. Chassaing, A.T. Gewirtz, Gut microbiota, low-grade inflammation, and metabolic syndrome, Toxicol. Pathol. 42 (1) (2014) 49–53.
[5] L. Catrysse, G.V. Loo, Inflammation and the metabolic syndrome: the tissue-specific functions of NF-κB, Trends Cell Biol. 27 (6) (2017) 417–429.
[6] G. Chen, H. Wang, X. Zhang, S.T. Yang, Nutraceuticals and functional foods in the management of hyperlipidemia, CRC Crit. Rev. Food Sci. Nutr. 54 (9) (2014) 1180–1201.
[7] J.Y. Yin, H.X. Lin, J. Li, Y.X. Wang, S.W. Cui, S.P. Nie, M.Y. Xie, Structural characterization of a highly branched polysaccharide from the seeds of Plantago asiatica L, Carbohydr. Polym. 87 (4) (2012) 2416–2424.
[8] L. Ren, C. Perera, Y. Hemar, Antitumor activity of mushroom polysaccharides: a review, Food Funct. 3 (11) (2012) 1118–1130.
[9] Y. Yu, M. Shen, Q. Song, J. Xie, Biological activities and pharmaceutical applications of polysaccharide from natural resources: a review, Carbohydr. Polym. 183 (2018) 91–101.
[10] S. Li, J. Li, G. Mao, T. Wu, Y. Hu, X. Ye, T. Ding, R.J. Linhardt, S. Chen, A fucoidan from sea cucumber *Pearsonothuria graeffei* with well-repeated structure alleviates gut microbiota dysbiosis and metabolic syndromes in HFD-fed mice, Food Funct. 9 (2018) 5371–5380.
[11] T. Zhang, Y. Yang, Y. Liang, X. Jiao, C. Zhao, Beneficial effect of intestinal fermentation of natural polysaccharides, Nutrients 10 (8) (2018) 1055.
[12] W.U. Nian, S. Chen, Y.E. Xingqian, L.I. Guoyun, L.A. Yin, C. Xue, Identification of Fucans from four species of sea cucumber by high temperature ~1H NMR, J. Ocean U. China 13 (5) (2014) 871–876.
[13] S. Chen, C. Xue, L.A. Yin, Q. Tang, G. Yu, W. Chai, Comparison of structures and anticoagulant activities of fucosylated chondroitin sulfates from different sea cucumbers, Carbohydr. Polym. 83 (2) (2011) 688–696.
[14] L. Zhao, M. Wu, C. Xiao, L. Yang, L. Zhou, N. Gao, Z. Li, J. Chen, J. Chen, J. Liu, Discovery of an intrinsic tenase complex inhibitor: pure nonasaccharide from fucosylated glycosaminoglycan, Proc. Natl. Acad. Sci. U. S. A. 112 (27) (2015) 8284.
[15] S.W. Hu, Y.G. Chang, J.F. Wang, C.H. Xue, Z.J. Li, Y.M. Wang, Fucosylated chondroitin sulfate from sea cucumber in combination with rosiglitazone improved glucose metabolism in the liver of the insulin-resistant mice, Biosci. Biotechnol. Biochem. 77 (11) (2013) 2263–2268.
[16] S. Hu, Y. Chang, J. Wang, C. Xue, D. Shi, H. Xu, Y. Wang, Fucosylated chondroitin sulfate from Acaudina molpadioides improves hyperglycemia via activation of PKB/GLUT4 signaling in skeletal muscle of insulin resistant mice, Food Funct. 4 (11) (2013) 1639.
[17] S. Hu, H. Xu, R. Chen, J. Wang, Z. Li, J. Xu, Activation of PKB and ERK, but not PI3K, is involved in fucosylated chondroitin sulphate from Acaudina molpadioides induced glucose uptake, J. Funct. Foods 10 (3) (2014) 385–396.
[18] Z. Zhu, B. Zhu, Y. Sun, C. Ai, L. Wang, C. Wen, J. Yang, S. Song, X. Liu, Sulfated polysaccharide from sea cucumber and its depolymerized derivative prevent obesity in association with modification of gut microbiota in high-fat diet-fed mice, Mol. Nutr. Food Res. (2018), 1800446. https://doi.org/10.1002/mnfr.201800446.
[19] N. Wu, Y. Zhang, X. Ye, Y. Hu, T. Ding, S. Chen, Sulfation pattern of fucose branches affects the anti-hyperlipidemic activities of fucosylated chondroitin sulfate, Carbohydr. Polym. 147 (2016) 1–7.
[20] S. Chen, G. Li, N. Wu, X. Guo, N. Liao, X. Ye, D. Liu, C. Xue, W. Chai, Sulfation pattern of the fucose branch is important for the anticoagulant and antithrombotic activities of fucosylated chondroitin sulfates, BBA-Gen. Subjects 1830 (4) (2013) 3054–3066.
[21] S. Chen, Y. Hu, X. Ye, G. Li, G. Yu, C. Xue, W. Chai, Sequence determination and anticoagulant and antithrombotic activities of a novel sulfated fucan isolated from the sea cucumber Isostichopus badionotus, BBA-Gen. Subjects 1820 (7) (2012) 989–1000.
[22] Y. Hu, S. Li, J. Li, X. Ye, T. Ding, D. Liu, J. Chen, Z. Ge, S. Chen, Identification of a highly sulfated fucoidan from sea cucumber Pearsonothuria graeffei with well-repeated tetrasaccharides units, Carbohydr. Polym. 134 (2015) 808–816.
[23] X. Guo, X. Ye, Y. Sun, D. Wu, N. Wu, Y. Hu, S. Chen, Ultrasound effects on the degradation kinetics, structure, and antioxidant activity of sea cucumber Fucoidan, J. Agric. Food Chem. 62 (5) (2014) 1088–1095.
[24] Y. Sun, X. Yang, X. Lu, D. Wang, Y. Zhao, Protective effects of Keemun black tea polysaccharides on acute carbon tetrachloride-caused oxidative hepatotoxicity in mice, Food Chem. Toxicol. 58 (3) (2013) 184–192.
[25] K.J. Livak, T.D. Schmittgen, Analysis of relative gene expression data using real-time quantitative PCR and the $2^{-\Delta\Delta CT}$ method, Methods 25 (4) (2001) 402–408.
[26] C.C. Evans, K.J. Lepard, J.W. Kwak, M.C. Stancukas, S. Laskowski, J. Dougherty, L. Moulton, A. Glawe, Y.W. Wang, V. Leone, D.A. Antonopoulos, D. Smith, E.B. Chang, M.J. Ciancio, Exercise prevents weight gain and alters the gut microbiota in a mouse model of high fat diet-induced obesity, PLoS One 9 (3) (2014), e92193.
[27] Z. Ling, Z. Li, X. Liu, Y. Cheng, Y. Luo, X. Tong, L. Yuan, Y. Wang, J. Sun, L. Li, Altered fecal microbiota composition associated with food allergy in infants, Appl. Environ. Microbiol. 80 (8) (2014) 2546–2554.
[28] J. Corbett, C. Mathews, Metabolic disorders and inflammation, Drug Discov. Today 3 (3) (2006) 365–366.
[29] R.G. Baker, M.S. Hayden, S. Ghosh, NF-kappaB, inflammation, and metabolic disease, Cell Metab. 13 (1) (2011) 11–22.
[30] A.M. Minihane, S. Vinoy, W.R. Russell, A. Baka, H.M. Roche, K.M. Tuohy, J.L. Teeling, E.E. Blaak, M. Fenech, D. Vauzour, Low-grade inflammation, diet composition and health: current research evidence and its translation, Br. J. Nutr. 114 (7) (2015) 999–1012.
[31] A.G. Cristancho, M.A. Lazar, Forming functional fat: a growing understanding of adipocyte differentiation, Nat. Rev. Mol. Cell Biol. 12 (11) (2011) 722.
[32] J.M. Olefsky, C.K. Glass, Macrophages, inflammation, and insulin resistance, Annu. Rev. Physiol. 72 (2010) 219–246.
[33] H. Cao, Adipocytokines in obesity and metabolic disease, J. Endocrinol. 220 (2) (2014) T47.
[34] B.O.V. Shum, C.R. MacKay, C.Z. Gorgun, M.J. Frost, R.K. Kumar, G.S. Hotamisligil, M.S. Rolph, The adipocyte fatty acid–binding protein aP2 is required in allergic airway inflammation, J. Clin. Invest. 116 (8) (2006) 2183–2192.
[35] W. Khazen, J.P. M'Bika, C. Tomkiewicz, C. Benelli, C. Chany, A. Achour, C. Forest, Expression of macrophage-selective markers in human and rodent adipocytes, FEBS Lett. 579 (25) (2005) 5631–5634.
[36] Y. Luo, C.M. Burrington, E.C. Graff, J. Zhang, R.L. Judd, P. Suksaranjit, Q. Kaewpoowat, S.K. Davenport, A.M. O'Neill, M.W. Greene, Metabolic phenotype and adipose and liver features in the high fat Western diet-induced mouse model of obesity-linked NAFLD, Am. J. Phys. 310 (6) (2016) E418.

[37] A.M. Valdes, J. Walter, E. Segal, T.D. Spector, Role of the gut microbiota in nutrition and health, BMJ 361 (2018), k2179.
[38] S.F. Clarke, E.F. Murphy, K. Nilaweera, P.R. Ross, F. Shanahan, P.W. O'Toole, P.D. Cotter, The gut microbiota and its relationship to diet and obesity: new insights, Gut Microbes 3 (3) (2012) 186–202.
[39] G. Chen, M. Xie, Z. Dai, P. Wan, H. Ye, X. Zeng, Y. Sun, Kudingcha and Fuzhuan brick tea prevent obesity and modulate gut microbiota in high-fat diet fed mice, Mol. Nutr. Food Res. 62 (6) (2018), 1700485.
[40] C.A. Lozupone, J.I. Stombaugh, J.I. Gordon, J.K. Jansson, R. Knight, Diversity, stability and resilience of the human gut microbiota, Nature 489 (7415) (2012) 220–230.
[41] H. Wang, X. Zhang, S. Wang, H. Li, Z. Lu, J. Shi, Z. Xu, Mannan-oligosaccharide modulates the obesity and gut microbiota in high-fat diet-fed mice, Food Funct. 9 (2018) 3916–3929.
[42] P.J. Turnbaugh, R.E. Ley, M.A. Mahowald, V. Magrini, E.R. Mardis, J.I. Gordon, An obesity-associated gut microbiome with increased capacity for energy harvest, Nature 444 (7122) (2006) 1027–1031.
[43] H. Zeng, S.L. Ishaq, F.-Q. Zhao, A.-D.G. Wright, Colonic inflammation accompanies an increase of β-catenin signaling and Lachnospiraceae/ Streptococcaceae bacteria in the hind gut of high-fat diet-fed mice, J. Nutr. Biochem. 35 (2016) 30–36.
[44] J. Bai, Y. Zhu, Y. Dong, Modulation of gut microbiota and gut-generated metabolites by bitter melon results in improvement in the metabolic status in high fat diet-induced obese rats, J. Funct. Foods 41 (2018) 127–134.
[45] N.O. Kaakoush, Insights into the role of Erysipelotrichaceae in the human host, Front. Cell. Infect. Microbiol. 5 (2015) 84.
[46] B.W. Parks, E. Nam, E. Org, E. Kostem, F. Norheim, S.T. Hui, C. Pan, M. Civelek, C.D. Rau, B.J. Bennett, Genetic control of obesity and gut microbiota composition in response to high-fat, high-sucrose diet in mice, Cell Metab. 17 (1) (2013) 141–152.
[47] N.D. Schwalm, E.A. Groisman, Navigating the gut buffet: control of polysaccharide utilization in *Bacteroides* spp, Trends Microbiol. 25 (12) (2017) 1005–1015.
[48] G.A. Weiss, C. Chassard, T. Hennet, Selective proliferation of intestinal Barnesiella under fucosyllactose supplementation in mice, Br. J. Nutr. 111 (9) (2014) 1602–1610.